B.7.2 S2 and S4 - Upper and Lower Horn Angle

The horn angle is the angle made by a line drawn from the leading edge to the peak thickness point as shown in Figure B8. A horn angle of 180 degrees would be a 'horn' pointing directly upstream. Angles for the cylinder cases may be in error because there was no reference mark on the test cylinder to indicate the horizontal, so it may be that the template was rotated with respect to the horizontal for some of the ice shape tracings.

Figure B9 shows the S2 (Upper Horn Angle) values for runs ID 1 through 6 - the glaze cases. Higher angle numbers indicate more forward horns and vice versa. Again, template rotation may have affected horn placement.

Figure B10 shows the S4 (Lower Horn Angle) parameter for runs ID 1 through 6 - the glaze cases. Lower numbers indicate more forward horns and vice versa. Template rotation may have affected horn placement.

Figure B11 shows the S4 parameter for runs ID 7 through 11 - the rime cases. This parameter has been relabeled "Maximum Forward Thickness Angle" because the rime shapes don't have real horns. An angle of 180 degrees marks the horizontal position. Angles greater than 180 degrees are below the stagnation point and vice versa. Template rotation may have affected these results.

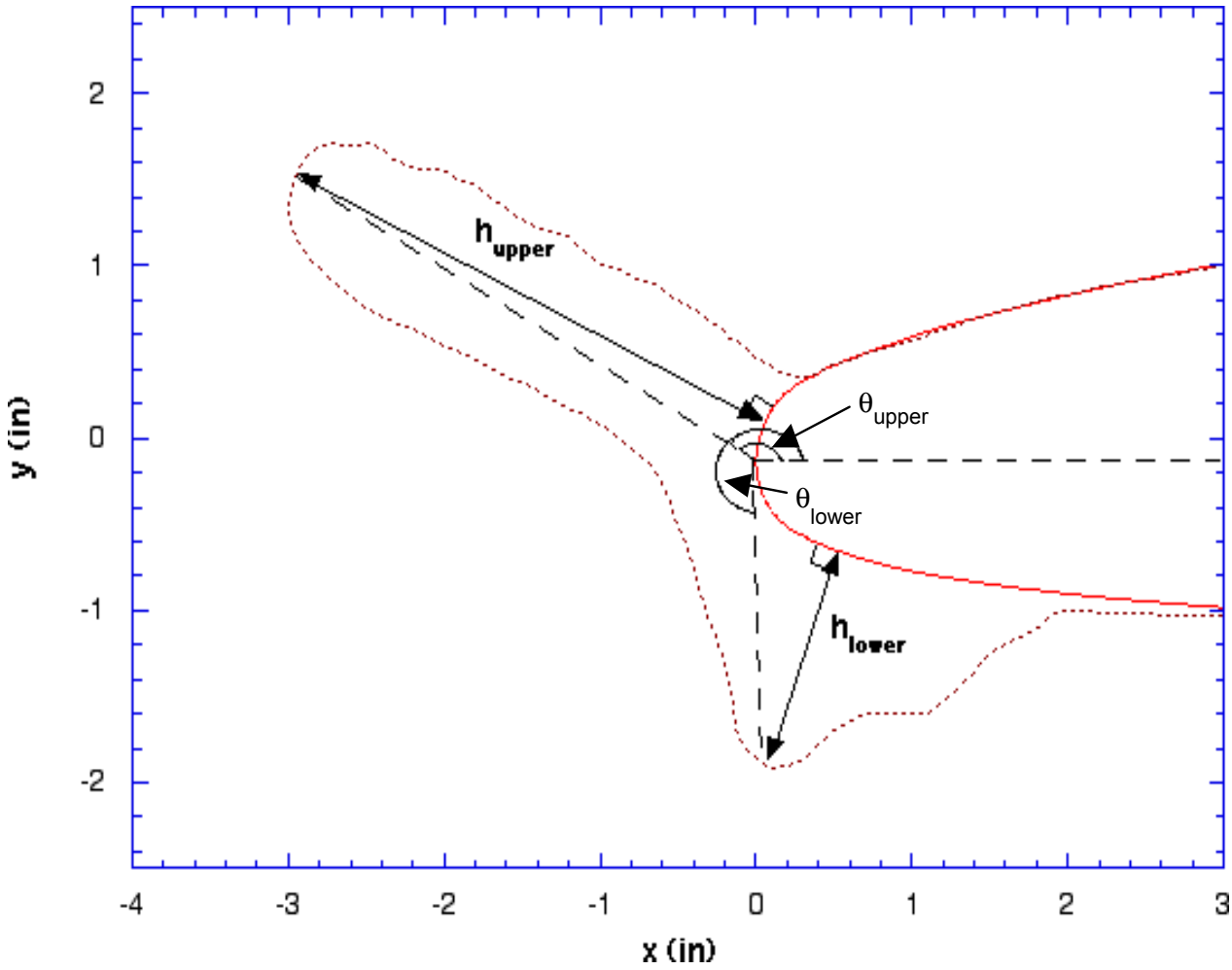

FIGURE B8 - HORN ANGLE DEFINITION

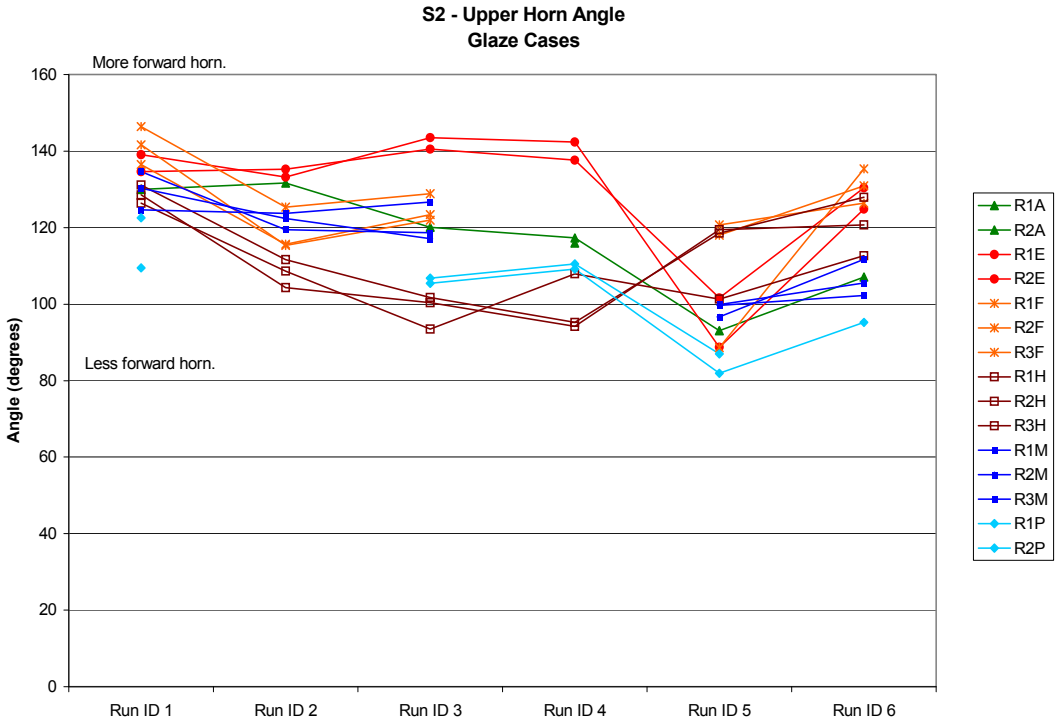

FIGURE B9 - S2 - GLAZE CASES

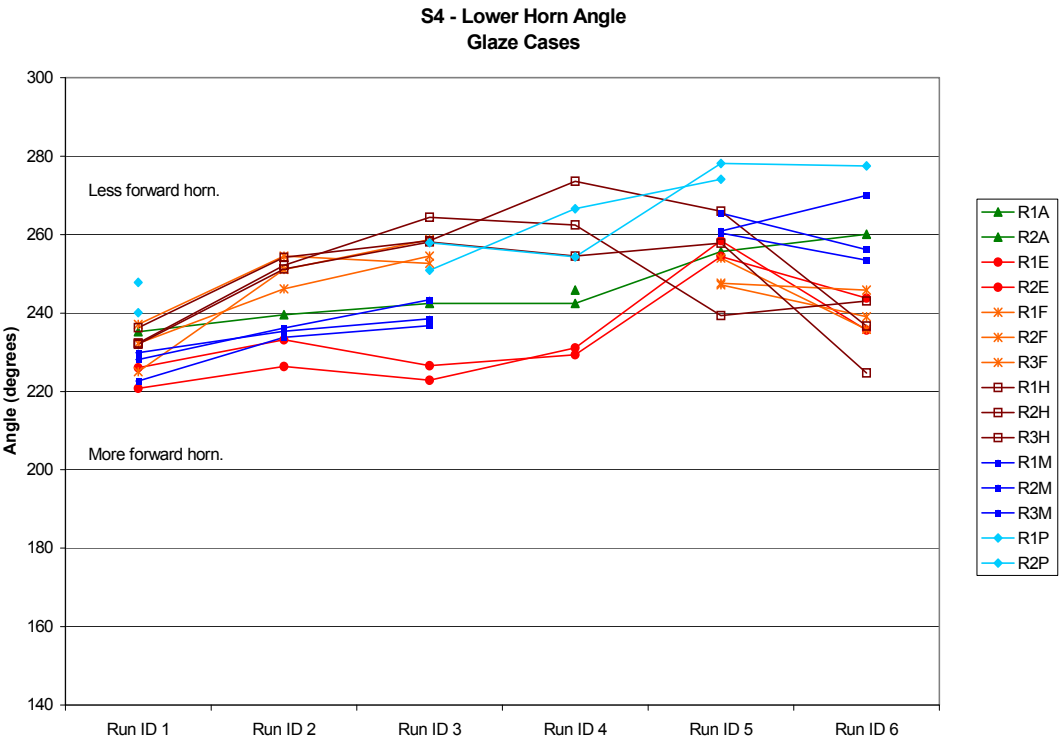

FIGURE B10 - S4 - GLAZE CASES

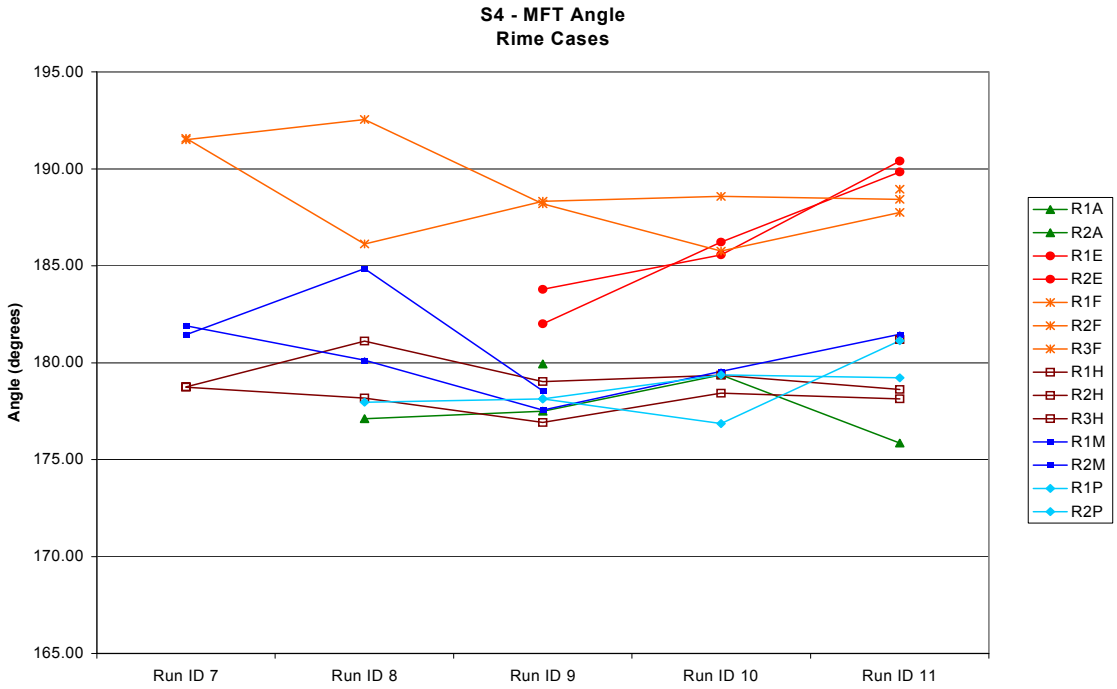

FIGURE B11 - S4 - RIME CASES

B.7.3 S5 - Total Ice Area

The total ice area is found by integrating the area of the airfoil plus ice shape and subtracting the airfoil area. The ice area is found from the wrapped plots, so anomalies in the unwrapped plots do not affect these values.

An estimate of the ice area can be obtained from Equation B4.

$$\text{Estimated Area} = A_c E d^2 \qquad \text{(Eq. B4)}$$

where:

A_c = the accumulation parameter given by Equation B3

E = the total collection efficiency

d = the cylinder diameter

Although E can be obtained from programs such as LEWICE, the values used in the present work were derived from the plot of K_0 vs. E in DOT/FAA/CT-88/8-I, Aircraft Ice Accretion Section.

Figure B12 shows the S5 (Total Ice Area) parameter for run ID 1 through 6 - the glaze cases - with the estimated area given by Equation B4 included. (In this and subsequent figures the estimated area curve is included as an additional point of reference in assessing trends in the ice area data. The formula should NOT be regarded as providing “truth.”] The ice areas for Tunnel H are greater than those for all the other tunnels.

Although the estimated area is basically in the middle of the test results for the LWC = 0.5 g/m^3 cases, it is generally higher than the test results (ignoring Tunnel H) for the LWC = 1.0 g/m^3 cases.

Figure B13 shows the S5 (Total Ice Area) parameter for run ID 7 through 11 - the rime cases - with the estimated area included. Again, the ice areas for Tunnel H are greater than those for the other tunnels. The estimated area tracks well with the test results (ignoring Tunnel H results).

B.7.4 S6 - Leading Edge Minimum Thickness

The leading edge minimum thickness, as calculated by THICK, is really the minimum between the two horns that THICK has chosen. It is calculated from the unwrapped plot and is not necessarily at the leading edge. Therefore, it might not be the appropriate thickness if THICK has chosen the horns badly or if THICK has introduced anomalies into the unwrapped plot. Only one such case was encountered in the cylinder data so, the data were manually corrected.

Figure B14 shows the S6 (Leading Edge Minimum Thickness) parameter for run ID 1 through 6 - the glaze cases, with the incorrect Tunnel H value replaced by the correct leading edge minimum value.

B.7.5 S7 and S8 - Upper and Lower Icing Limits

A normal line is projected out from each point on the airfoil. The first and last such points which intersect the ice shape are considered the icing limits. Note that if there are “overhangs” in the ice shape, the icing limits chosen by THICK may be aft of the actual ice locations on the clean shape. Figure B15 shows the S7 (Upper Icing Limit) parameter for run ID 1 through 6 - the glaze cases. Figure B16 shows the S8 (Lower Icing Limit) parameter for run ID 1 through 6 - the glaze cases. Figure B17 shows the S7 (Upper Icing Limit) parameter for run ID 7 through 11 - the rime cases. Figure B18 shows the S8 (Lower Icing Limit) parameter for run ID 7 through 11 - the rime cases.

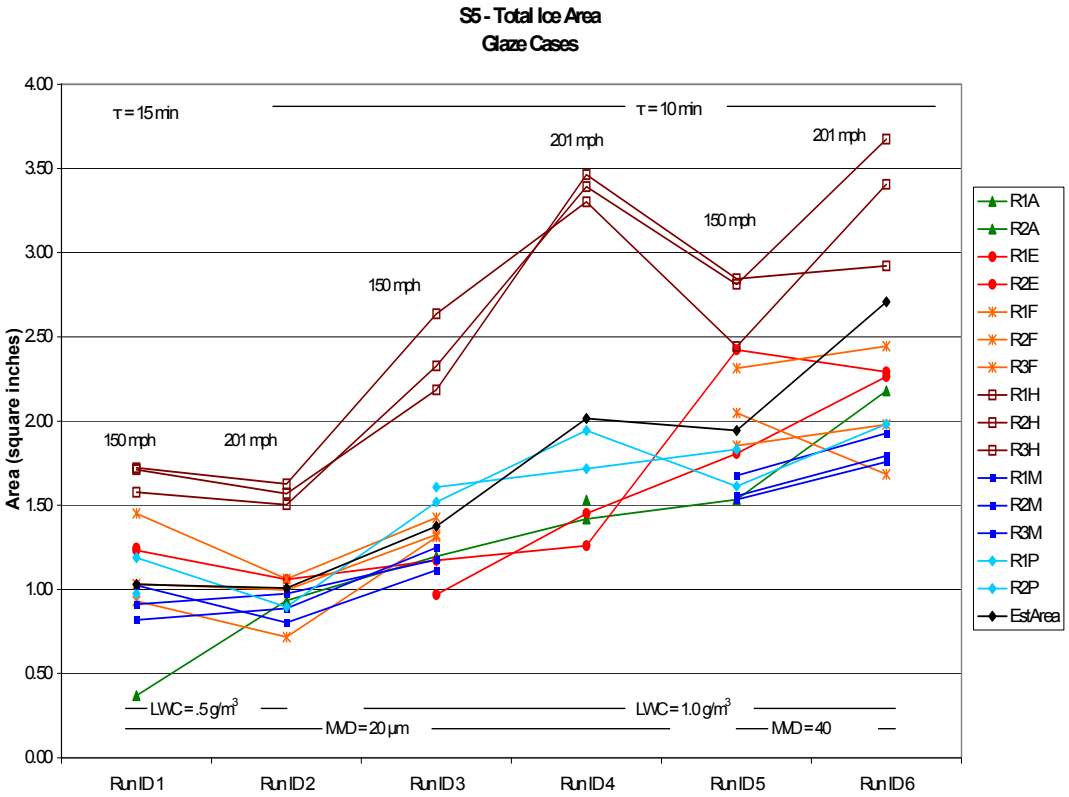

FIGURE B12 - S5 - GLAZE CASES

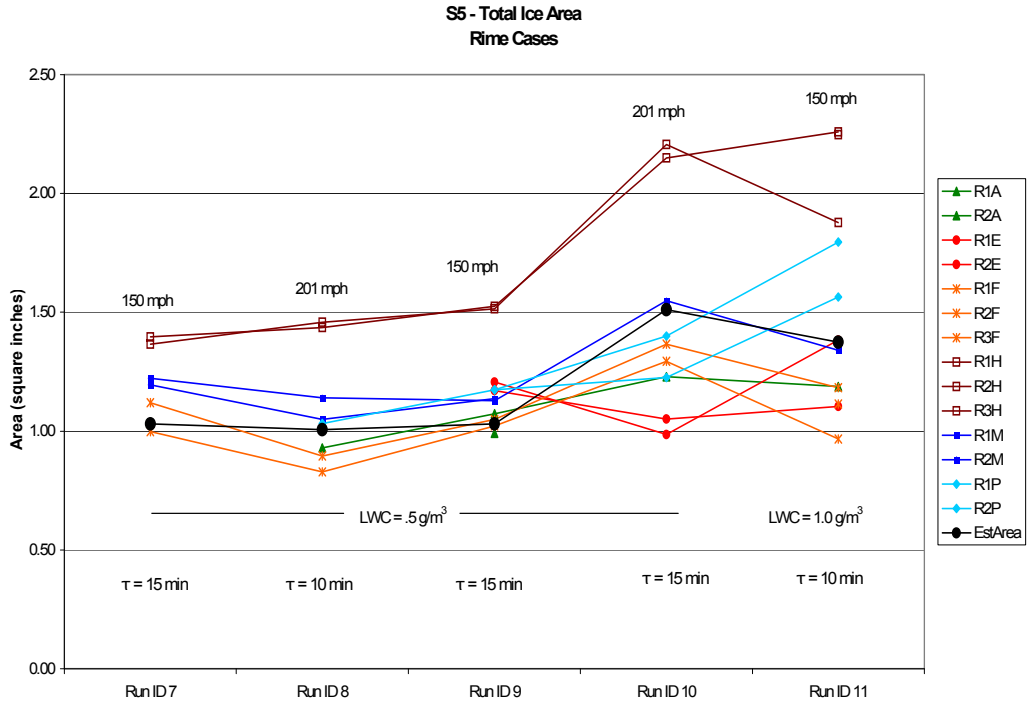

FIGURE B13 - S5 - RIME CASES

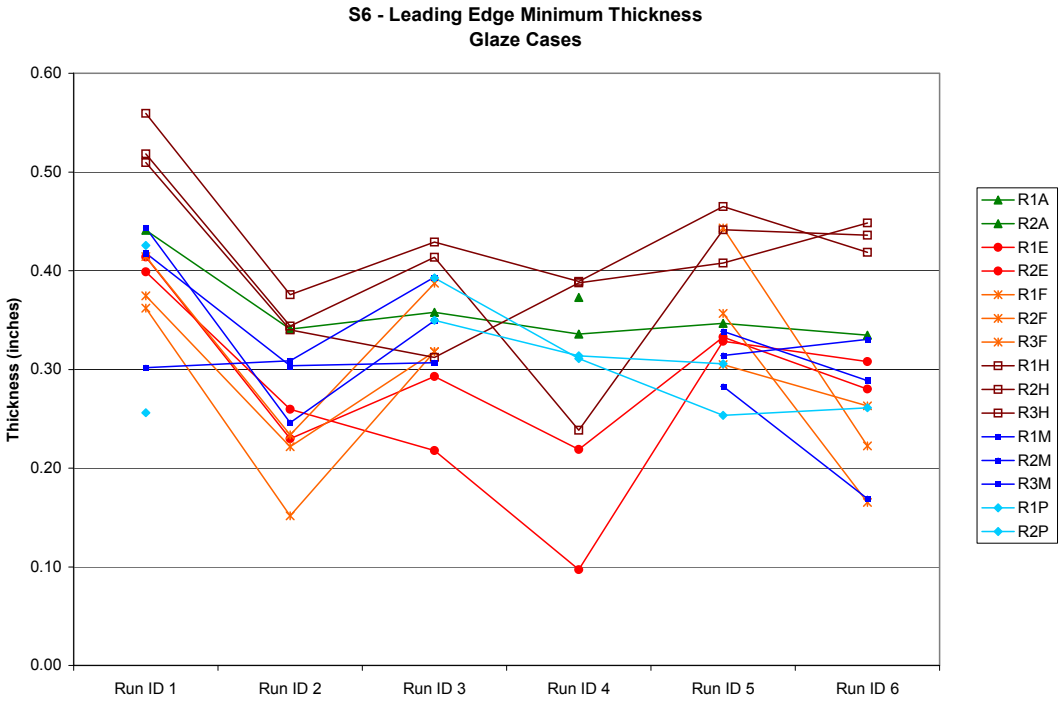

FIGURE B14 - S6 - GLAZE CASES WITH ANOMALOUS POINT REPLACED

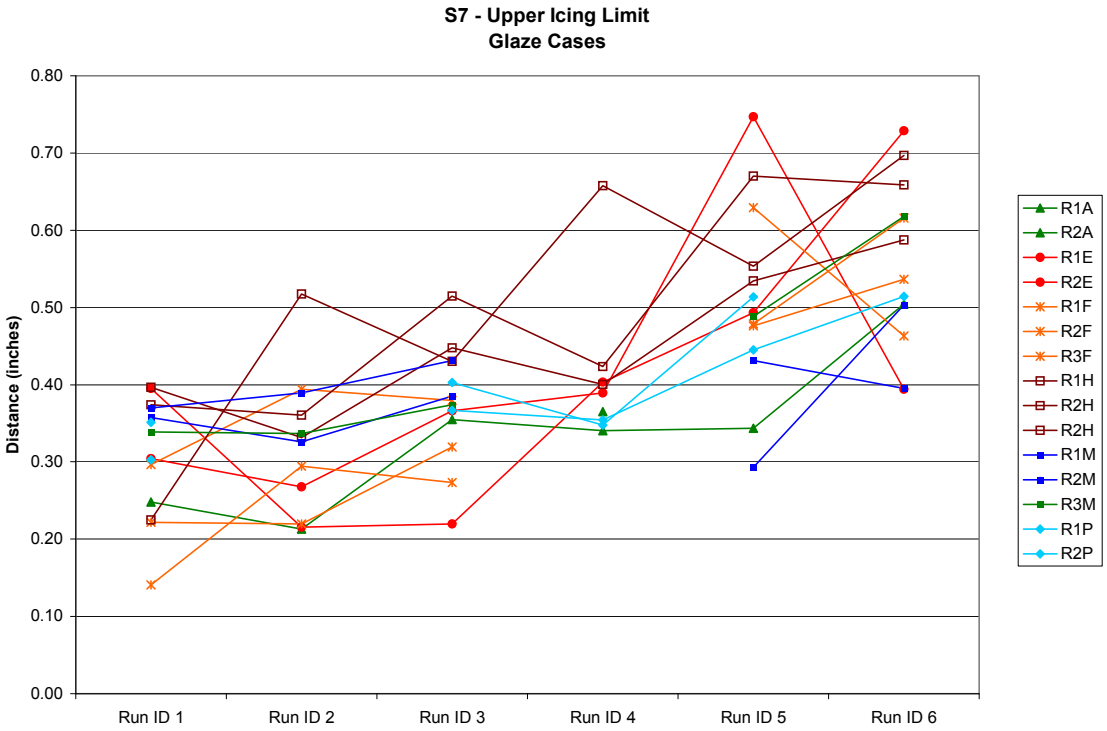

FIGURE B15 - S7 - GLAZE CASES

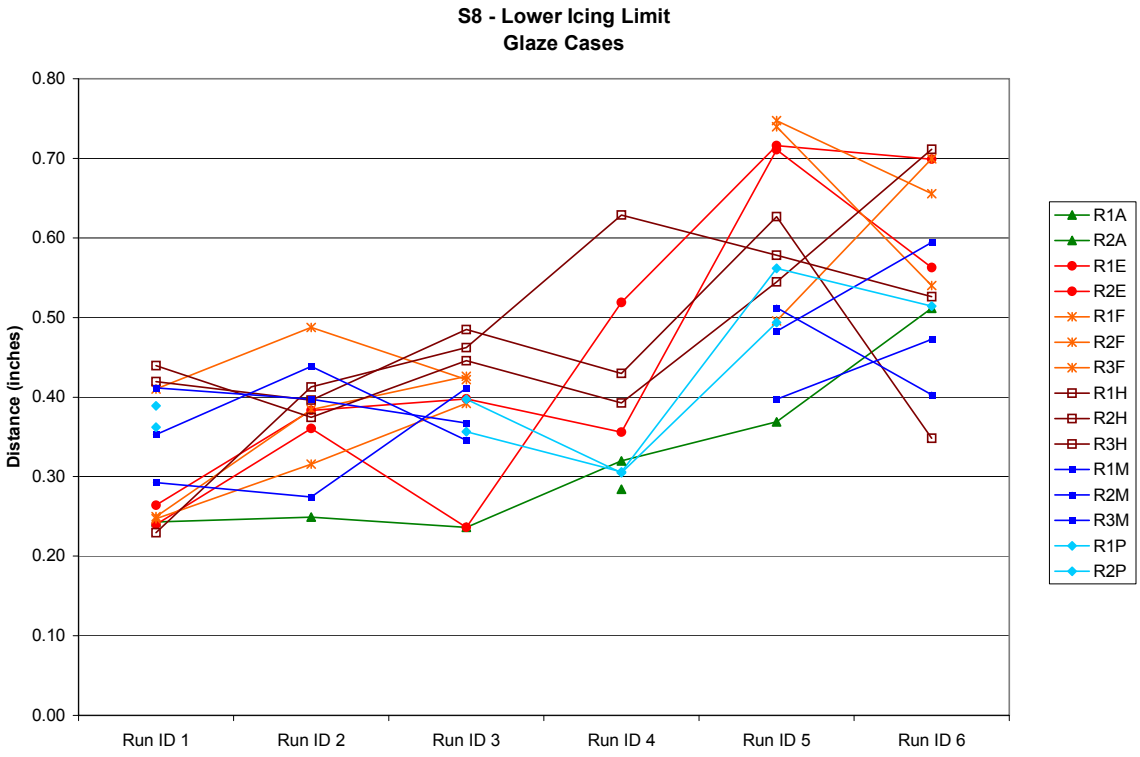

FIGURE B16 - S8 - GLAZE CASES

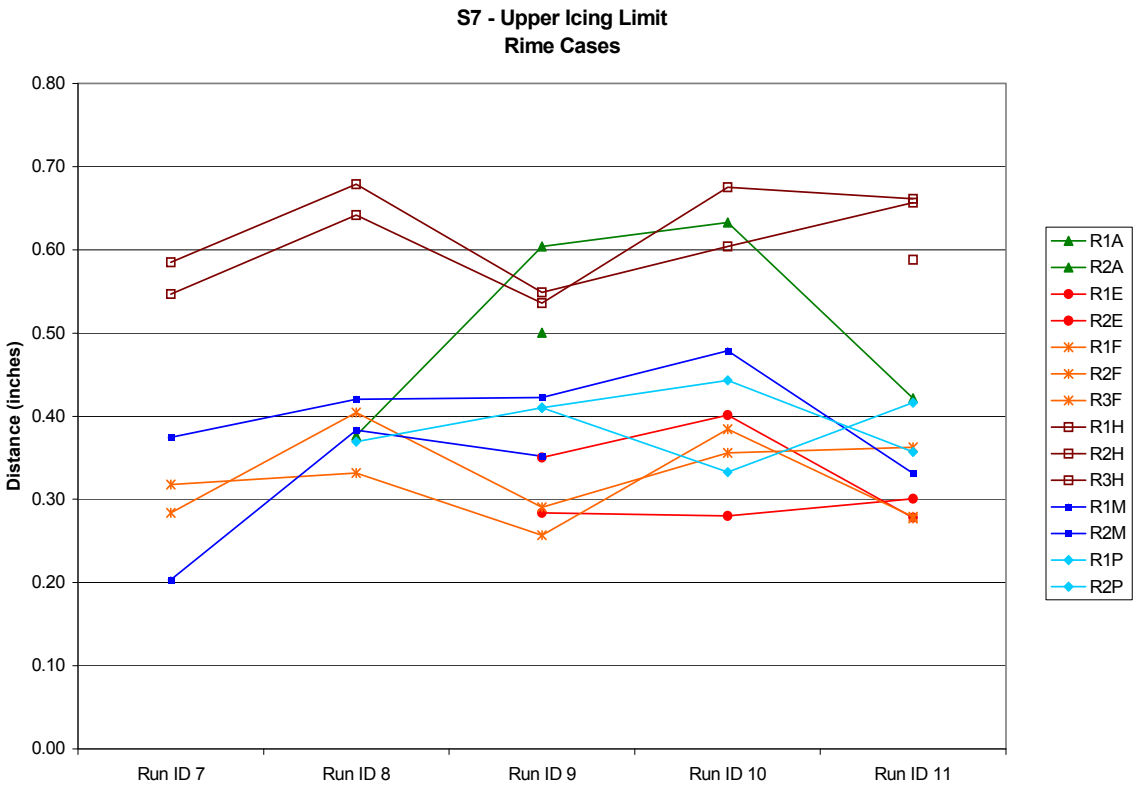

FIGURE B17 - S7 - RIME CASES

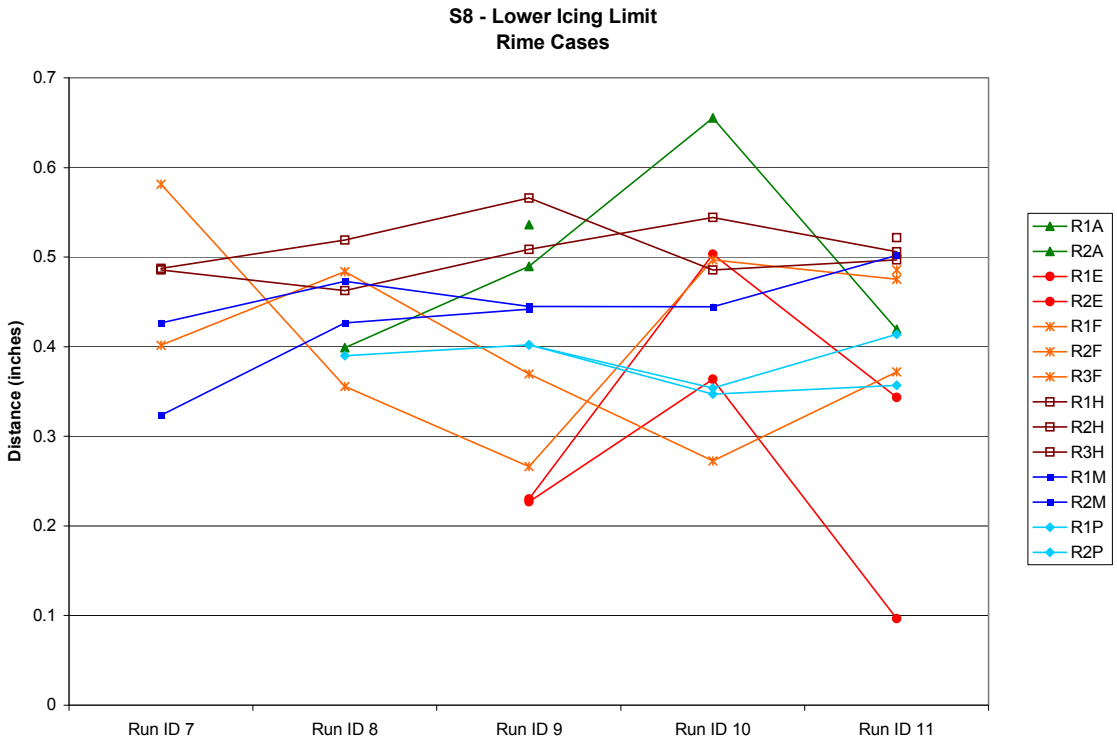

FIGURE B18 - S8 - RIME CASES

B.8 PROPOSED NEW PARAMETERS

The cylinders used for these tests do not have a reference mark to identify the absolute horizontal position. Therefore, as has been noted, testers may have rotated the template with respect to its correct position on the cylinder, thereby causing a rotation in the resulting ice shape tracing. If two tracings have about the same number of degrees between the upper and lower horns, but the horns themselves are displaced, this could indicate a rotation of the template rather than an actual difference in horn locations on the ice shapes. This comparison could only be implemented for the glaze cases.

Figure B19 shows the angular difference between the upper and lower horn for each tunnel run. It appears that this parameter is more suited to identifying repeatability of tunnel results rather than rotation.

B.9 CONCLUSIONS

THICK results support the earlier assessment that there are substantial facility to facility discrepancies in ice shapes. They also provide good quantitative measures of the discrepancies. Plots show that trends in the ice thickness and ice area parameters are generally consistent among the facilities and with the theoretical formulae.

The parameters proposed to identify tracing template rotation fail to do so.

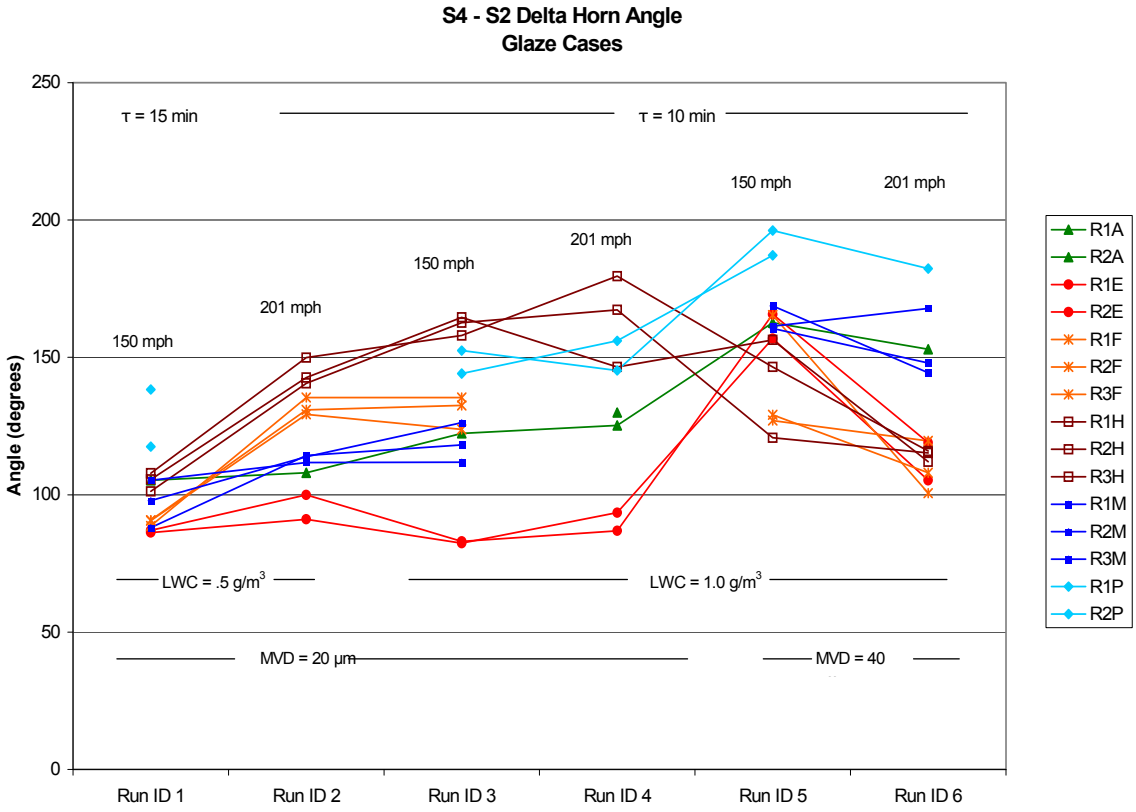

FIGURE B19 - DIFFERENCE BETWEEN UPPER AND LOWER HORN ANGLES- FREEZING FRACTION ANALYSIS

APPENDIX C

C.1 NOMENCLATURE

A_c Accumulation parameter, dimensionless

b Relative heat factor, dimensionless

c Airfoil chord, cm

c_p Specific heat of air, cal/g K

$c_{p,ws}$ Specific heat of water at the surface temperature, cal/g K

CL Tunnel centerline (mid-span) position

d Twice the leading-edge radius for airfoils, or diameter for cylinders, cm. For Equation C10, cylinder radius is substituted for d

D_v Diffusivity of water vapor, cm^2/sec

h_c Convective heat-transfer coefficient, $cal/s\,m^2\,K$

h_G Gas-phase mass-transfer coefficient, $g/s\,m^2$

k_a Thermal conductivity of air, $cal/s\,m\,K$

K Inertia parameter, dimensionless

K_0 Modified inertia parameter, dimensionless

LWC Cloud liquid-water content, g/m^3

MVD Water drop median volume diameter, μm

n_0 Stagnation freezing fraction, dimensionless

$n_{0,a}$ Freezing fraction calculated using Messinger analysis, dimensionless

$n_{0,e}$ Freezing fraction from stagnation ice thickness, dimensionless

Nu Nusselt number, dimensionless

p Static pressure, Nt/m^2

p_w Vapor pressure of water in atmosphere, Nt/m^2

p_{ww} Vapor pressure of water at the icing surface, Nt/m^2

r Recovery factor, dimensionless

Re Reynolds number of model, dimensionless

Re_δ Reynolds number of water drop, dimensionless

Sc Schmidt number, dimensionless

t_f Freezing temperature of water, °C

t_s Surface temperature, °C

t Temperature, °C

T Absolute temperature, K

V Free-stream velocity of air, m/s

β_0 Stagnation collection efficiency, dimensionless

Δ_0 Ice thickness at stagnation line, cm

ϕ Water drop energy transfer parameter, °C

λ Water drop range, m

λ_{Stokes} Water drop range if Stokes Law applies, m

Λ_f Latent heat of freezing of water, cal/g

Λ_v Latent heat of evaporation of water, cal/g

μ Viscosity of air, g/m s

θ Air energy transfer parameter, °C

ρ Air density, g/m^3

ρ_i Ice density, g/m^3

ρ_w Liquid water density, g/m^3

τ Accretion time, min

Subscripts

st Static

tot Total